Pergamon

Journal of Structural Geology, Vol. 16, No. 9, pp. 1275 to 1281, 1994

0191-8141/94 $07.00+0.00

0191-8141(94)E0002-G

Evidence for a non-linear relationship between fracture spacing and layer thickness

NIBIR MANDAL, SANJITENDRA KRISHNA DEB and DEBDARPAN KHAN

Department of Geological Sciences, Jadavpur University, Calcutta 700 032, India

(*Received* 23 *September* 1992; *accepted in revised form* 23 *November* 1993)

Abstract—In experiments, extension fractures were generated in rigid layers of Plaster of Paris resting on a viscous substratum (pitch). The experimental results predict a non-linear relationship between the spacing of fractures in uniform brittle layers and layer thickness for fractures generated by the tractional force of embeddins weak rocks. We derive an equation which relates the critical fracture spacing (λ_c) with layer thickness (b), tensile strength of the layer material/viscosity of the embedding medium ratio (τ_0/η) and bulk strain rate ($\dot{\epsilon}_b$). The equation shows that the spacing increases as a function of the square root of the layer thickness. The theory also predicts that the fracture spacing depends on the strain rate when the embedding weak medium is viscous.

INTRODUCTION

IN ROCKS of contrasting lithologies, the competent layers often have fractures or joints that are more or less regularly spaced. Such fractures may develop either in response to tensile stresses exerted by the flow of less competent layer, as for example in boudinaged structures (Ramberg 1955) or in response to internal tensile stresses generated within the layers, e.g. cooling joints (Hyndman 1985, p. 66) and mud cracks (Pettijohn 1975, p. 122).

Statistical analyses of fracture or joint spacing in a mechanical layer show a characteristic frequency distribution (Huang & Angelier 1989, Narr & Suppe 1991) which is weakly skewed and follows a gamma-distribution function or near log-normal distribution. Also, the median of joint spacing distribution increases with the mechanical layer thickness (Narr & Suppe 1991). Several investigations (Price 1966, Hobbs 1967, Sowers 1973, Narr & Suppe 1991) revealed that fracture spacing depends on mechanical layer thickness, on contrast in strengths between the fractured layer and the embedding medium, on layer-parallel extensional strain and on the presence of pre-existing flaws.

Although the increase in fracture spacing with increase in layer thickness is well documented, the exact quantitative relationship between layer thickness and fracture spacing is not well established. Some workers (Bodgonov 1947, Novikova 1947, Price 1966, Narr & Suppe 1991) have suggested a linear relationship between them. However, such a linear relationship is not universally accepted (Norris 1966, Mastella 1972). Joint spacing in thicker beds shows a non-linear relationship (Ladeira & Price 1981).

Using theory and experiments, the present study explores the relationship of fracture spacing with layer thickness, the ratio of tensile strength for the fracturing layer to the viscosity of embedding medium, and bulk strain rate of the system. Both the theoretical and experimental results indicate that, under layer-parallel extension, a set of fractures will develop more or less simultaneously at a mechanically most-favoured spacing. In such a situation fracture spacing will have a non-linear relationship to mechanical layer thickness.

FRACTURE SPACING IN ANALOG MODELS

Experimental method

The experiments were conducted with rigid layers of Plaster of Paris resting on a ductile substratum of pitch (Fig. 1). The rigid layers were prepared in the following manner. A volume of Plaster of Paris powder was mixed with water to form a dense liquid. The liquid was then poured into a rectangular box on the pitch block and allowed to dry under the air of a fan. A soft solid layer formed when the water in the liquid evaporates after drying for a certain interval of time. The borders of the layers were cut out with a knife and the rectangular box was removed (Fig. 1b). The layer became rigid and its tensile strength increased progressively with further drying. The tensile strength of layer could, thus, be qualitatively controlled by the time of drying. For example, layers with large tensile strengths were created by drying periods of 15–20 min before beginning an experiment. In contrast, layers with lower tensile strength were generated by 4–6 min of drying.

The rigid layers fractured in response to extension of the ductile substratum. Two sets of experiments were conducted. In the first series of experiments, the thicknesses of layers were varied while the tensile strength of the material was unchanged. In the second series of experiments, tensile strength of the material was increased while the layer thickness remained constant. Similar experiments yielded similar results indicating the reproducibility of the experimental procedure.

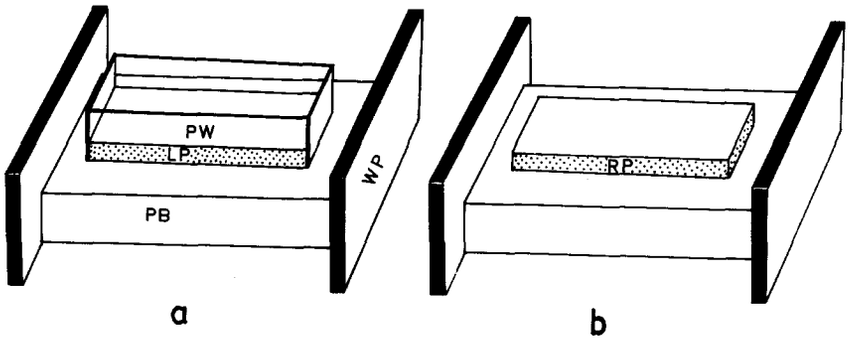

Fig. 1. (a) A sketch of experimental set-up. PB—pitch block, LP—liquid Plaster of Paris, PW—Perspex-walled box, WP—wooden plate. (b) Same set-up after removal of the Perspex-walled box when the liquid Plaster of Paris has solidified, RP—rigid layer of Plaster of Paris.

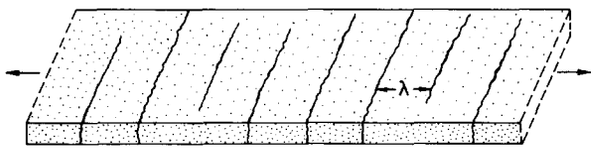

Fig. 2. Mode of development of fractures in three dimensions in a layer of Plaster or Paris. Fracture spacing (λ) was measured on the plan of the model. Arrows show bulk tension direction.

Experimental results

Under layer-parallel tension, a set of mode I (extension) fractures nucleated more or less simultaneously in the brittle Plaster of Paris layer. However, the fractures were not strictly arranged in a line. Some fractures nucleated in the central part and propagated to the borders of the model while fractures propagated from the margins to the centre in some other places. The propagation of fractures took place in a plane at a right angle to the bulk extension direction. In course of progressive extension, most of the fractures very rapidly transected the entire width of the Plaster of Paris strip. However, at any instant there were always some fractures that did not extend the entire width (Fig. 2). The incomplete fracture propagation resulted in certain degree of non-uniformity in the spacing in profile of the model. Thus, the fracture spacing was measured from the surface of the model that yielded a very consistent regular value (Fig. 2).

In the experiments with rigid layers of the same strength but different thicknesses, the fractures were closely spaced in the thin layers while they were more widely spaced in the thicker layers (Fig. 3a). These experiments yielded comparable magnitudes of layer thickness vs fracture spacing ratio with respect to field data (Ladeira & Price 1981, Narr & Suppe 1991). For example, the average spacing of fractures is about 0.9 cm when the layer has a thickness of 0.22 cm, whereas spacing increases to 2.85 cm when the thickness is 0.85 cm. However, the fracture spacing does not increase linearly with the layer thickness (Fig. 4). The experimental curve for the non-linear variation is very similar to the curves of spacing vs bed thickness for field joints (fig. 2 in Ladeira & Price 1981).

In the second set of experiments fracture spacing in the layers of higher tensile strength was always higher than that in a layer of lower tensile strength for a given thickness (Fig. 3b).

THEORETICAL ANALYSIS

The present experiments show that the fractures in a layer are initiated all over the model more or less simultaneously at a regular spacing. None of the experiments displayed development of fractures by successive halving of the layers. This observation indicates that, under layer-parallel tension a rigid layer of large extent fails by a set of fractures which is mechanically most favoured. As was found in previous work (Hobbs 1967, Pollard & Segall 1987, Narr & Suppe 1991), these experiments show that layer thickness and tensile strength are important parameters for determining fracture spacing. In the following section, a theory will be developed that shows the strain rate of the system as an important additional factor when the embedding medium is viscous.

Mathematical derivation

A set of fractures will develop at a mechanically most favoured spacing where the resistance of the rigid layer to the bulk extension is minimal. The resistive forces act in two ways: resistance to layer failure and boundary resistance to the flow of weaker matrix at the surface of the rigid layer. To analyse these resistive forces, consider a uniform and flawless rigid layer of infinite extent resting on a viscous substratum with viscosity, η, where the system is extended by a bulk strain rate, $\dot{\varepsilon}_b$. Let a co-ordinate frame (Fig. 5) be chosen such that the x axis is parallel to the extension direction and lies on the surface of the layer. Considering the first type of resistance, the tangential force at any point on the rigid layer (cf. equation 15 of Mandal & Khan 1991) is

$$T_x = A \cdot x, \tag{1}$$

where T_x is tractional force of the embedding medium on unit surface area of the rigid layer, x is the point of interest on the layer and A is a constant to be evaluated from the boundary conditions of the present problem. For convenience let a segment of the rigid layer with width, λ, be considered with one boundary at $x = 0$ and

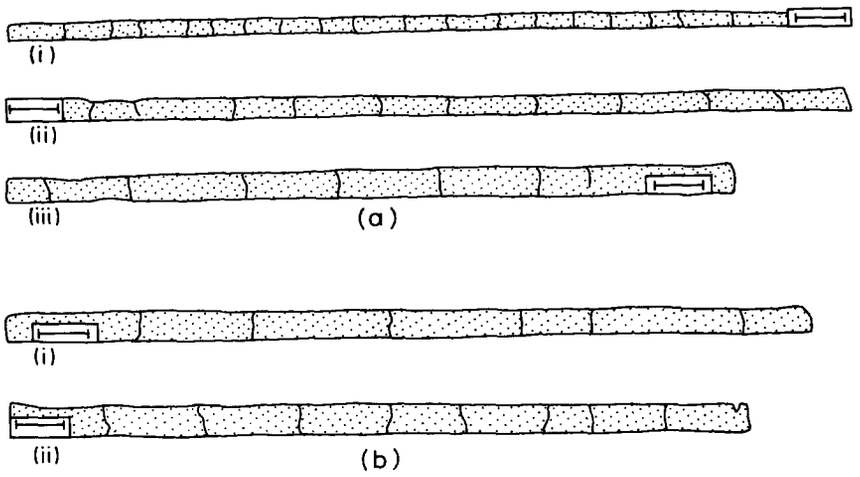

Fig. 3. Tensional fractures in layers of Plaster of Paris. (a) Layers of different thicknesses: (i) 0.22, (ii) 0.39 and (iii) 0.57 cm, etc., but similar strength. (b) Layers of different strengths but about same thickness, 0.63 cm: layer (i) is harder than layer (ii). Scale bar = 1 cm.

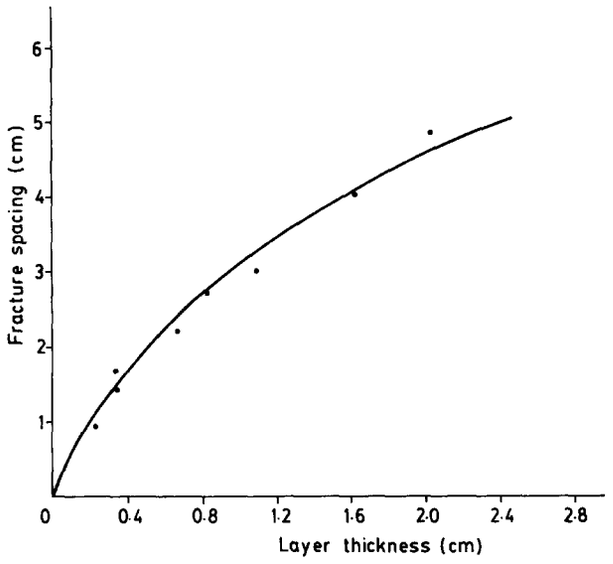

Fig. 4. Plot of fracture spacing vs layer thickness from experiments with layers of different thicknesses but similar rigidity (Fig. 3a).

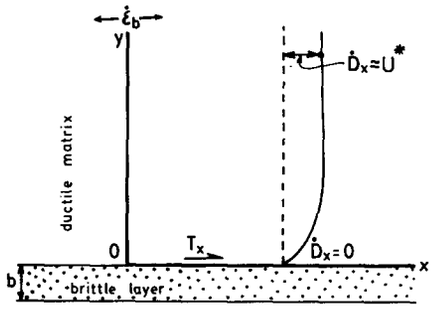

Fig. 5. Co-ordinate frame (xy) with x axis parallel to the bulk extension direction and lying on the interface of the brittle layer. Variation of the displacement rate ($\dot{D}_x$) along the x direction of points on a line (dashed) parallel to the y axis is shown by the solid line. b is the layer thickness, $\dot{\varepsilon}_b$ is the bulk extension rate of the embedding medium. T_x is tangential force per unit area at any point x on the surface of the layer. U^* is the far-field velocity in the x direction.

the other at $x = \lambda$. Assuming that the tensile force causing fracturing is a result of the tangential force, the tensile force F_x may be determined from equation (1)

$$F_x = 2\int_0^{\lambda} T_x \, dx = 2\int_0^{\lambda} A \cdot x \cdot dx = A \cdot \lambda^2. \quad (2)$$

For extension fracturing at $x = 0$ by the tensile force F_x the following condition must be satisfied (Ramberg 1955).

$$F_x = \tau_o \cdot b, \quad (3)$$

where τ_o and b are tensile strength and layer thickness, respectively. Substituting equation (2) in equation (3) we get

$$A = \tau_o \cdot b/\lambda^2. \quad (4)$$

During fracture initiation at $x = 0$, the resistive force on the layer surface at $x = \lambda$ will be, from equation (1),

$$T_\lambda = \tau_o \cdot b/\lambda. \quad (5)$$

Equation (5) shows that, during fracture initiation at $x = 0$, the resistive force decreases with increasing distance (λ) from the initiation site. The analysis indicates that fractures form more easily at a greater spacing.

Consider next the second resistance to fracturing from the weaker viscous interbeds at the interface with the fracturing layer. A flow gradient forms in the bedding-parallel velocity. A drag resistance to the bulk flow of the matrix results. The variation of displacement rate $\dot{D}_x$ for a line parallel to the y axis (Fig. 5) may be represented by the following equation that satisfies the boundary conditions, $\dot{D}_x \to U^*$ when $y \to \infty$ and $\dot{D}_x \to 0$ as $y \to 0$:

$$\dot{D}_x = U^*\{1 - \exp(-y/\eta^k)\}, \quad (6)$$

where U^* is the x component of the velocity of a particle in the matrix, where drag resistance is absent, relative to the velocity of a particle at the layer interface ($\dot{D}_x = 0$, Fig. 5). η is the matrix viscosity and k is an arbitrary positive constant. In this equation η^k is a factor because

drag resistance depends on viscosity. For example, a zone of drag resistance will be wide when the viscosity is large and narrow when the latter is very low. At any point the velocity gradient in the y direction can be determined by differentiating equation (6) as

$$\frac{d\dot{D}_x}{dy} = \frac{U^*}{\eta^k} \cdot \exp(-y/\eta^k). \tag{7a}$$

At the layer interface $y = 0$

$$\frac{d\dot{D}_x}{dy} = \frac{U^*}{\eta^k}. \tag{7b}$$

In the present theoretical analysis the matrix is assumed to be linearly viscous, so the shear is proportional to the velocity gradient. Thus, flow resistance adjacent to the layer interface is

$$T_r = \eta \cdot \frac{d\dot{D}_x}{dy} \tag{8}$$

(Douglas *et al.* 1990).

Substituting for $d\dot{D}_x/dy$ from equation (7b)

$$T_r = \eta^{1-k} \cdot U^*.$$

Taking $U^* = x \cdot \dot{\varepsilon}_b$, where $\dot{\varepsilon}_b$ is the far-field longitudinal strain rate parallel to the layering,

$$T_r = \eta^{1-k} \cdot x \cdot \dot{\varepsilon}_b. \tag{9}$$

From equation (9) the resistance to the matrix flow at $x = \lambda$ is

$$T_r = \eta^{1-k} \cdot \dot{\varepsilon}_b \cdot \lambda. \tag{10}$$

For fractures to be initiated at $x = 0$ and $x = \lambda$ the total resistance to the bulk extension of the system at $x = \lambda$ is obtained by summing equations (5) and (10):

$$T_R = T_\lambda + T_r$$

$$T_R = \tau_o \cdot b/\lambda + \eta^{1-k} \cdot \dot{\varepsilon}_b \cdot \lambda. \tag{11}$$

Equation (11) shows that T_R increases with both a decrease and increase in λ. Thus a critical λ value should exist at which T_R is a minimum. Differentiating equation (11) to determine the minimum,

$$\frac{\partial T_R}{\partial \lambda} = -\frac{\tau_o \cdot b}{\lambda_c^2} + \eta^{1-k} \cdot \dot{\varepsilon}_b = 0 \tag{12}$$

$$\frac{\tau_o \cdot b}{\lambda_c^2} = \eta^{1-k} \cdot \dot{\varepsilon}_b$$

$$\lambda_c^2 = \frac{\tau_o \cdot b}{\eta^{1-k} \cdot \dot{\varepsilon}_b}$$

$$\lambda_c = \left\{\left(\frac{\tau_o}{\eta^{1-k}}\right) \cdot \left(\frac{1}{\dot{\varepsilon}_b}\right) \cdot b\right\}^{1/2}, \tag{13}$$

where λ_c is the critical spacing for two consecutive fractures that involves a minimum resistance to the bulk extension of the layered system. Equation (13) shows that the critical spacing increases non-linearly with layer thickness. The theoretical curve for spacing vs thickness (Fig. 6) for $\tau_o = 1.56$ Pa, $\eta = 1.5 \times 10^6$ poise and $\dot{\varepsilon}_b = 10^{-1}\ s^{-1}$ resembles the curve obtained from experimental data (Fig. 4). The shapes of fracture spacing vs thickness curves change with changes in the rheological parameters τ_o, η. Figure 6 shows that the curves for the lower range of τ_o are gentle and show a lesser variation in fracture spacing with layer thickness. On the other hand, the curves for higher τ_o values, other parameters remaining constant, are steep and show non-linearity for a wide range of layer thickness. The increase in fracture spacing with layer thickness can also be analysed by differentiating equation (13) with respect to layer thickness,

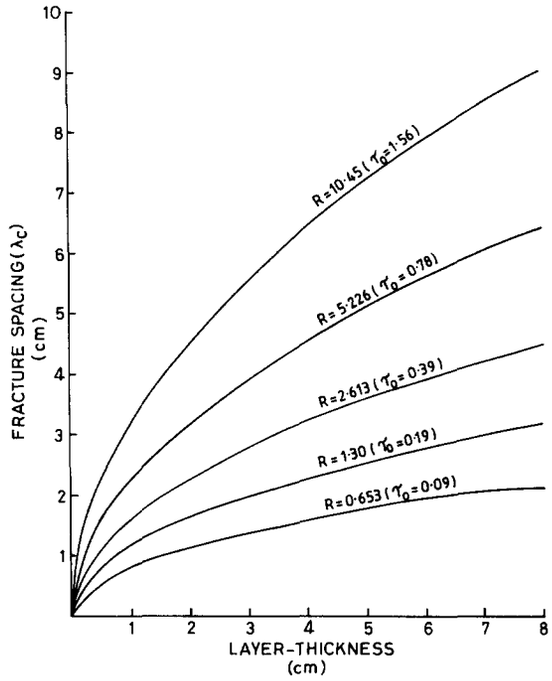

Fig. 6. Fracture spacing (λ_c) vs layer thickness (b) relationship (from equation 13) for different R values where $R = (\tau_o\ \eta^{1-k})\ (1/\dot{\varepsilon}_b)$. The corresponding τ_o values in Pa are given in brackets while η and $\dot{\varepsilon}_b$ are kept constant and have values of 1.5×10^6 poise and $10^{-1}\ s^{-1}$, respectively and $k = 0$.

$$\frac{\partial \lambda_c}{\partial b} = \frac{\sqrt{R}/2}{\sqrt{b}}, \tag{14}$$

where

$$R = \frac{\tau_o}{\eta^{1-k}} \cdot \frac{1}{\dot{\varepsilon}_b}.$$

From equation (14), the change in critical fracture spacing is small for large layer thickness (b). For very large thicknesses fracture spacing may appear to be independent of layer thickness as is seen in field data for spacing vs thickness (Ladeira & Price 1981).

Layer-parallel finite strain is not a parameter in equation (13). Thus, fracture spacing does not depend on extension magnitude but on the bulk strain rate ($\dot{\varepsilon}_b$) when the embedding weaker medium is viscous. Equation (13) indicates that fracture spacing decreases with increasing strain rate in the weaker viscous interbeds (Fig. 7).

The exponential function with an arbitrary constant k

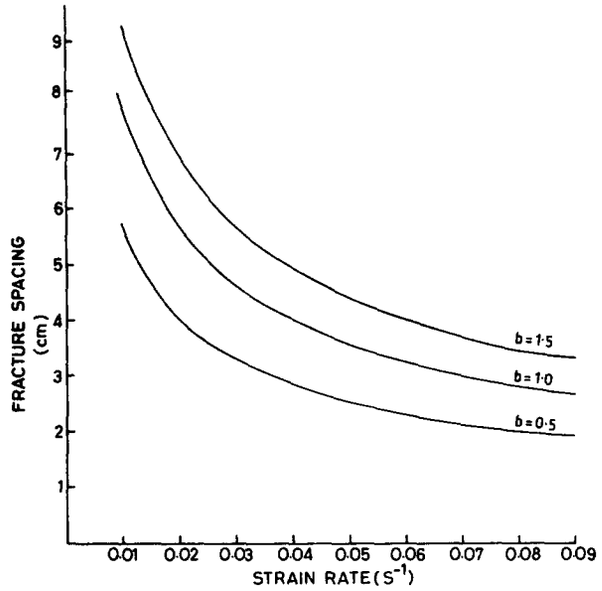

Fig. 7. Variation of fracture spacing with strain rate for different layer thicknesses (b) (from equation 13). τ_o, η are kept constant and have values of 1.0 Pa and 1.5×10^6 poise, respectively, and $k = 0$.

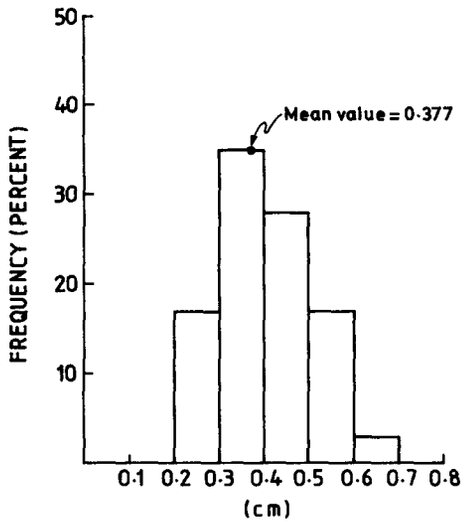

Fig. 8. Histogram for the fracture spacing distribution in a film-like thin layer of Plaster of Paris. Note that the mean value is close to the modal value of the distribution.

in equation (6) has been used to describe an asymptotic variation in velocity in a laminar flow on a rigid plate (fig. 135 in Streeter 1948, p 247). k needs to be characterized empirically. It is consistent with the observation that if viscosity (η) of embedding medium is high, velocity ($\dot{D}_x$) will approach the far-field value (U^*) gradually and over a large distance (y). Equation (10) shows that k will be less than 1 because at a given strain rate, shear stress exerted by higher viscosity materials is higher than that exerted by lower viscosity ones. Thus, in the present theoretical analysis we can only predict that k will lie in the range of 0–1. Equation (13) shows that λ_c is a monotonic function of k. Since $0 \leq k \leq 1$, the lowest fracture spacing could be at $k = 0$:

$$(\lambda_c)_L = \left\{\left(\frac{\tau_o}{\eta}\right) \cdot \left(\frac{1}{\dot{\varepsilon}_b}\right) \cdot b\right\}^{1/2}. \quad (15)$$

The arbitrariness of k gives a constraint in the direct application of the equation to field data. However, the prime aim of the analysis is to show fracture spacing as a non-linear function of bed thickness rather than to quantify it exactly. Equation (13) shows that for any finite value of k the function has a non-linear expression.

DISCUSSION AND CONCLUSIONS

The present study considers fracture spacing vs layer thickness relationships in rheologically contrasted rock sequences. Natural analogs include fractures in boudinaged stiff layers such as dolomite beds in phyllites, fractures in chert layers in limestones and, perhaps under some situations, joints in sandstone layers embedded in shales. In these natural settings the weaker embedding rocks tend to flow at a higher strain rate than the stiffer layers, thereby causing an interfacial traction. When the stiffer layer is brittle, it fractures in response to the traction (Ramberg 1955). The present experimental and theoretical results indicate that fracture spacing in these situations will necessarily show a non-linear relationship with layer thickness. This analysis will not be valid, however, for the fractures or joints generated

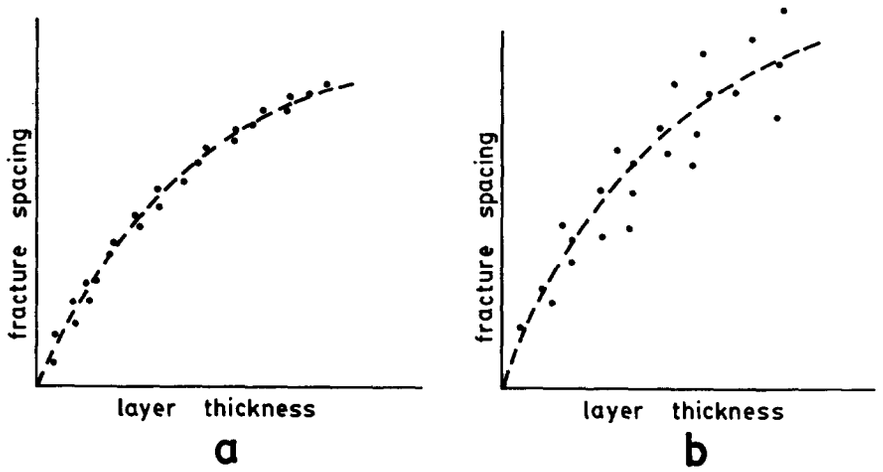

Fig. 9. Hypothetical curves for fracture spacing vs layer thickness variation: (a) an ideal situation with points following a smooth curve; (b) dispersion of points in a non-ideal situation where pre-existing flaws control fracture initiation sites.

by stresses acting within the brittle later, e.g. hydraulic pressure. In such cases, fracture spacing may be independent of layer thickness (Ladeira & Price 1981).

In the experiments the fractures initiated in response to layer-parallel extension were of purely tensional type. In conformity with the experiments the present analysis considers the spacing vs thickness relationship for purely tensile fractures. Thus, the analysis considers tensile strength of the brittle layer. The tensile strength is directly equated (equation 3) with layer-parallel traction at which the brittle layer fails (Ramberg 1955). However, for other modes of failure of the brittle layer (shear or hybrid fracture) the present analysis could also be applicable after some modifications. For this, critical tensile stress (σ_T) at which the brittle layer fails is to be determined from a Mohr circle construction. The Mohr circle with σ_T and layer-normal compression (σ_N) will touch the stability curve for the brittle layer. The layer-normal compression for the present case is $-\eta\cdot\dot{\varepsilon}_b$. Then, in equation (13) τ_o is to be replaced by σ_T.

The fractures in the experiments are more or less regularly spaced and do not show a large variation in the spacing in any one experimental model. However, fracture spacing distributions are not so regular in rocks. Some workers have used median (Narr & Suppe 1991) or mode (Rives *et al.* 1992) for analyses of fracture spacing distributions. Since the present experimental models were small in size, the number of fractures in a layer was not large. So we considered a simple arithmetic mean spacing as has been used by Ladeira & Price (1981) in field. However, we also conducted experiments with film-like thin layers of Plaster of Paris that produced numerous fractures, the spacing distribution of which is slightly asymmetric, somewhat similar to field data (Narr & Suppe 1991). But the mean value is close to the modal value of the distribution (Fig. 8). Thus, we infer that in the present analysis of fracture spacing in experiments, using mean values does not lead to significant errors.

The present analysis and experimental data indicate that when regular fractures develop at a mechanically favoured spacing, a non-linear relationship occurs between fracture spacing and layer thickness. In the analysis fracturing layers are assumed flawless and uniform in thickness. The present results may deviate where pre-existing inhomogeneities are abundant (Jaegar 1969, p. 215, Adams & Sines 1978). The presence of flaws causes lowering in tensile strength of fracturing layers locally (Narr & Suppe 1991). If such flaws are statistically uniform in distribution, fractures can also grow systematically from the flaws. From equation (13) the spacing at which the flaws in the layer will be activated would depend upon the effective tensile strength, which would be controlled by the flaw length at a given strain rate in the embedding medium. Since the boundary traction remains constant for a constant extension rate after initiation of the mechanically favoured set of fractures further activation of flaws at a closer spacing will not take place because tensile stress in the layer segments is reduced. However, fracture spacing will necessarily show a non-linear relationship with the layer thickness as the flaws are activated mostly at a critical spacing (λ_c) and it will be qualitatively similar to the present results. In contrast, if the flaws are of varying lengths in the distribution, the development of fractures will be spatially irregular because effective tensile strength is different in different parts of a layer (Narr & Suppe 1991). For a given thickness, depending on the distribution of the flaws the spacing would vary. Thus field data may show fracture spacing vs layer thickness in a non-linear variation with wide dispersion of the points, instead of following the theoretically derived smooth curve (Fig. 9).

The present quantitative analysis indicates that fracture spacing depends on the bulk strain rate. So local deviations in strain rate may cause disturbances in the ideal relationship between layer thickness and fracture spacing. A local increase in the strain rate generates higher tractions and results in more close-spaced fractures locally. The spacing distribution in this type of situation may be asymmetric (cf. Narr & Suppe 1991) with its mode towards the lower value in the distribution.

The embedding material has been considered as a viscous substance. So the layer parallel traction is proportional to the strain rate that remains constant with progressive extension. If the embedding substance were elastic, its traction on the brittle layer would increase with progressive stretching and the tensile stress in a segment of the brittle layer would increase continuously (Hobbs 1967). Thus, at the instant when tensile stress reaches the tensile strength, a set of fractures would develop at a spacing as if under the stress for certain strain rate when the matrix is viscous. With further extension tensile stresses in each segment increase so as to reach the tensile strength again giving rise to another set of fractures at a lower spacing (Hobbs 1967). As a result fracture spacing will depend on the layer-parallel finite strain when the embedding weaker medium is elastic.

From the present study it is concluded that, in the rock sequences of contrasting rheology, fractures in the stiff layers of large lateral extent grow at a mechanically favoured spacing (involving minimum resistance in the bulk extension) in response to layer-parallel traction by the weaker interbeds. The fracture spacing (λ_c) is a function of layer thickness, the ratio of tensile strength of layer material to viscosity of the embedding medium and the bulk strain rate. Spacing does not depend on extensional strain magnitude if the embedding medium is viscous. Fracture spacing in this type of situation has a non-linear relationship to layer thickness and it is insensitive to layer thicknesses for large thicknesses.

Acknowledgements—We wish to thank Professor S. K. Ghosh for encouraging us to carry out the work. Professor S. F. Wojtal went through the manuscript with great care and provided us with a detailed outline for revising the manuscript. His contribution is deeply appreciated. We also wish to thank two anonymous reviewers, one of whom made many constructive criticisms that helped us to upgrade the manuscript. The present work was funded by the Council of Scientific and Industrial Research, India.

REFERENCES

Adams, M. & Sines, G. 1978. Crack extension from flaws in a brittle material subjected to compression. *Tectonophysics* **49**, 97–118.

Bodgonov, A. A. 1947. The intensity of cleavage as related to the thickness of beds. *Soviet Geol.* **16** (in Russian).

Douglas, J. F., Gasiorek, J. M. & Swaffield, J. A. 1990. *Fluid Dynamics* (2nd edn). English Language Book Society/Longman.

Hobbs, B. E. 1967. The formation of tension joints in sedimentary rocks: an explanation. *Geol. Mag.* **104**, 550–556.

Huang, Q. & Angelier, J. 1989. Fracture spacing and its relation to bed thickness. *Geol. Mag.* **126**, 355–362.

Hyndman, D. W. 1985. *Petrology of Igneous and Metamorphic Rocks*. McGraw-Hill, New York.

Jaeger, J. C. 1969. *Elasticity, Fracture and Flow with Engineering and Geological Applications*. Methuen & Co. Ltd. and Science Paperbacks, John Wiley & Sons, Inc., New York.

Ladeira, F. L. & Price, N. J. 1981. Relationship between fracture spacing and bed thickness. *J. Struct. Geol.* **3**, 179–183.

Mandal, N. & Khan, D. 1991. Rotation, offset and separation of oblique-fracture (rhombic) boudins: theory and experiments under layer-normal compression. *J. Struct. Geol.* **13**, 349–356.

Mastella, L. 1972. Interdependence of joint density and thickness of layers in the Phodale Flysch. *Bull. Acad. Pol. Sci. Ser. Geol. Geogr.* **20**, 187.

Narr, W. & Suppe, J. 1991. Joint spacing in sedimentary rocks. *J. Struct. Geol.* **13**, 1037–1048.

Norris, D. K. 1966. The mesoscopic fabric of rock masses about some Canadian coal mines. *Proc. 2nd Congr. Int. Soc. Rock Mech.* **1**, 191–198.

Novikova, A. C. 1947. The intensity of cleavage as related to the thickness of the bed. *Soviet Geol.* **16** (in Russian).

Pettijohn, F. J. 1975. *Sedimentary Rocks*. Harper & Row, New York.

Pollard, D. D. & Segall, P. 1987. Theoretical displacements and stresses near fractures in rock: with application to faults, joints, veins, dikes and solution surfaces. In: *Fracture Mechanics of Rocks* (edited by Atkinson, B. K.). Academic Press, London, 277–349.

Price, N. J. 1966. *Fault and Joint Development in Brittle and Semi-brittle Rock*. Pergamon Press, Oxford.

Ramberg, H. 1955. Natural and experimental boudinage and pinch-and-swell structures. *J. Geol.* **63**, 512–526.

Rives, T., Razack, M., Petit, J.-P. & Rawnsley, K. D. 1992. Joint spacing: analogue and numerical simulation. *J. Struct. Geol.* **14**, 925–937.

Sowers, G. M. 1973. Theory of spacing of extension fractures. *Engng Geol. Case Hist.* **9**, 27–53.

Streeter, V. L. 1948. *Fluid Dynamics*. McGraw-Hill, New York.